Fluorescent Nanoparticles

DOI: 10.1002/anie.200700803

Synthesis of Highly Fluorescent Gold Nanoparticles for Sensing Mercury(II)**

*Chih-Ching Huang, Zusing Yang, Kun-Hong Lee, and Huan-Tsung Chang**

Monolayer-protected metal nanoparticles (NPs) have gained a great deal of attention in the past decade because of their unique electronic properties and potential optical-sensing applications.[1] Gold nanoparticles (AuNPs) exhibit size-dependent surface plasmon resonance (SPR) absorption properties when their conducting electrons in both the ground and excited states are confined to dimensions smaller than the electron mean free path (ca. 20 nm).[2] This simple and practical theory predicts the spectra of AuNPs that have diameters larger than 3 nm, but fails for smaller particles.[2] Confinement of electrons within metallic nanostructures at sizes comparable to the Fermi wavelength of the electron (ca. 0.7 nm) results in electronic energy states that exhibit molecule-like transitions because the density of these states is too low to reproduce bulk metallic properties.[3] The photoluminescence (PL) quantum yields (QYs) of Au monolayer-protected clusters (MPCs) can be enhanced by up to eight orders of magnitude with respect to that of bulk gold (10^{-10}).[4] Alkanethiol-protected Au nanoclusters ranging in size from several atoms to small particles (smaller than 1.2 nm) fluoresce ($QY \approx 10^{-5}$–10^{-2}) in the blue to near-IR region.[4] Upon decreasing the sizes of homologous stabilizer-protected Au nanoclusters, the emission wavelength undergoes a blue shift.[3a,4f,5a,6]

Recently, AuNPs emitting stronger fluorescence signals than those of AuMPCs have been prepared.[5] With their exceptional fluorescence properties, these fluorescent AuNPs are also called Au nanodots. AuNPs that are encapsulated and stabilized by polyamidoamine (PAMAM) dendrimers or polyethylenimine (PEI) exhibit stable fluorescence properties and high QYs (greater than 10%), which probably result from the lower density of energy states present in the very small Au nanodots (smaller than Au_{31}), thus minimizing the number of internal nonradiative relaxation pathways. Additionally, the PAMAM dendrimer cage protects these nanodots from quenchers present in solution.

Although the fluorescence phenomena of AuMPCs and AuNPs have been recognized for some time, examples of their application to chemical sensing are rare, mainly because of problems associated with their chemical and fluorescence instability.[4d,7] Furthermore, it is difficult to prepare AuNPs with a small size distribution;[4f,6–9] note that their fluorescence behavior is highly size-dependent. Herein we report that the introduction of various alkanethiol ligands onto the surfaces of 2.9 (±0.5)-nm AuNPs can be used to control their fluorescence properties (excitation and emission wavelengths, as well as QY). In addition, we unveil a new homogeneous assay for the highly selective and sensitive detection of Hg^{II} ions; it is based on aggregation-induced quenching of the fluorescence of 11-mercaptoundecanoic acid (11-MUA) protected AuNPs (11-MUA-AuNPs; (2.0 ± 0.1) nm) in the presence of 2,6-pyridinedicarboxylic acid (PDCA).

Figure 1 displays high-resolution transmission electron microscopy (HRTEM) images of AuNPs and AuNPs capped with 2-mercaptoethanol (2-ME), 6-mercaptohexanol (6-MH), and 11-mercaptoundecanol (11-MU); these as-prepared alkanethiol-capped AuNPs are denoted as 2-ME-AuNPs, 6-MH-AuNPs, and 11-MU-AuNPs, respectively. The TEM images indicate that the particles are well-dispersed. The inset in Figure 1 A suggests that the lattice fringes of the as-prepared AuNPs are consistent with metallic gold having a discerned lattice spacing of 2.4 Å, which corresponds to the *d* spacing of

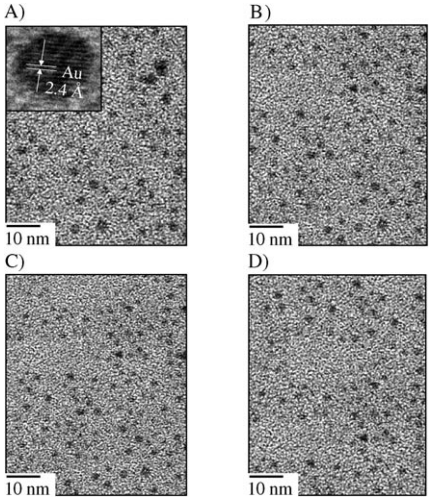

Figure 1. HRTEM images of A) AuNPs, B) 2-ME-AuNPs, C) 6-MH-AuNPs, and D) 11-MU-AuNPs.

[*] Dr. C.-C. Huang, Z. Yang, K.-H. Lee, Prof. H.-T. Chang
Department of Chemistry
National Taiwan University, 1, Section 4
Roosevelt Road, Taipei 106 (Taiwan)
Fax: (+886) 2-3366-1171
E-mail: changht@ntu.edu.tw.
Prof. H.-T. Chang
Department of Natural Science Education
National Taitung University
Taitung (Taiwan)

[**] This study was supported by the National Science Council of Taiwan under contracts NSC 95-2113-002-026-MY3. C.-C.H. acknowledges the PDF support from National Taiwan University.

Supporting information for this article is available on the WWW under http://www.angewandte.org or from the author.

the (111) crystal plane of fcc Au.[10] The average diameters of the four particles are 2.9 (±0.5), 2.3 (±0.3), 2.2 (±0.2), and 2.0 (±0.2) nm, respectively. This result indicates that the diameters of the particles decrease upon increasing the size of the thiol capping agent. Because of significant fragmentation energies, once the capping agents are adsorbed onto the particle surfaces, the AuNPs tend to dissociate into smaller Au and Au–thiolate clusters.[11] The smallest diameter for the 11-MU-AuNPs suggests greater degrees of breaking and detaching of larger-sized AuNP clusters and/or Au–thiol complexes.[11] The capping agents form very strong covalent, distinctly directional Au–S bonds on the AuNP surfaces and, thus, they stabilize the particles (clusters) in aqueous solution. The 2-ME-AuNPs, 6-MH-AuNPs, and 11-MU-AuNPs are all stable in aqueous solution at 4 °C for at least three months, considerably longer than the stability of the AuNPs (two days).

Figure 2 A displays the absorption spectra of the AuNP, 2-ME-AuNP, 6-MH-AuNP, and 11-MU-AuNP solutions. Because the average size of the as-prepared AuNPs was 2.9 nm, they exhibited no apparent absorption band

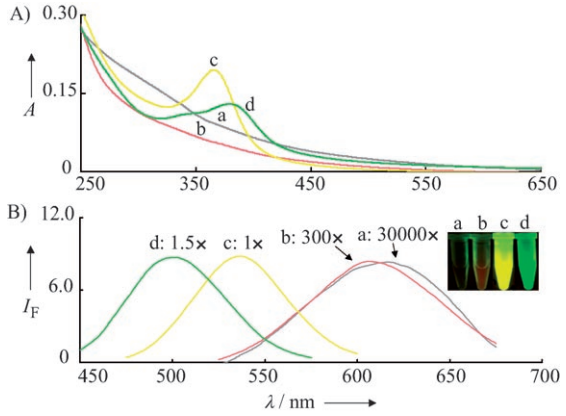

Figure 2. A) UV/Vis absorbance spectra and B) normalized fluorescence spectra of AuNPs (a), 2-ME-AuNPs (b), 6-MH-AuNPs (c), and 11-MU-AuNPs (d). Inset to (B): photograph of the fluorescence of the various AuNPs upon excitation under a hand-held UV lamp (365 nm). The normalized fluorescence intensities (I_F) are plotted in arbitrary units; excitation wavelength: 365 nm. The concentration ratio of the AuNPs, 2-ME-AuNPs, 6-MH-AuNPs, and 11-MU-AuNPs was 30000:300:1:1.5 in (B).

(curve a).[2] Similarly, there was no apparent absorption band for 2-ME-AuNPs. In contrast, the 6-MH- and 11-MU-AuNPs exhibited absorption-band maxima at wavelengths (λ_{max}^{abs}) of 367 ($\varepsilon = 2.76 \times 10^6\,M^{-1}\,cm^{-1}$) and 383 nm ($\varepsilon = 1.80 \times 10^6\,M^{-1}\,cm^{-1}$), respectively. According to the literature, the absorption bands for 6-MH- and 11-MU-AuNPs originate from metal-centered (Au $5d^{10}$ to 6sp interband transitions) and/or ligand–metal charge-transfer transitions.[4,12] The absorption spectral profiles of our 6-MH- and 11-MU-AuNPs closely resemble those of small Au MPCs and polynuclear gold(I) complexes, such as the Au clusters protected by glutathione, tiopronin, *meso*-2,3-dimercaptosuccinic acid, dodecanethiol, PEI, and PAMAM, each of which exhibit a broad absorption band centered within the wavelength range from 300 to 700 nm.[4,5]

Figure 2 B displays normalized fluorescence spectra of the as-prepared AuNP, 2-ME-AuNP, 6-MH-AuNP, and 11-MU-AuNP solutions. The inset indicates that the fluorescence colors of the four solutions upon excitation at 365 nm are dark brown, reddish, yellow, and green, respectively. Because the four particles possessed different fluorescence QYs, their fluorescence spectra are presented after normalization. The narrower emission profiles and smaller Stokes shifts for the 6-MH- and 11-MU-AuNPs, relative to those for the 2-ME-AuNPs, are mainly due to the former pair's narrower size distributions and lower degrees of distortion in the excited state.[5a] The QYs (Table 1) for the 11-MUA- and 2-ME-

Table 1: Optical properties of AuNPs and alkanethiol–AuNPs.

Au nanoparticle	λ_{max}^{abs} [nm]	λ_{max}^{em} [nm]	Emission FWHM [nm][a]	QY[b]
AuNPs	–[c]	618	90	1.0×10^{-6}
2-ME-AuNPs	–[c]	613	83	6.2×10^{-5}
TG-AuNPs[d]	–[c]	611	78	9.3×10^{-5}
4-MB-AuNPs[e]	–[c]	603	72	3.5×10^{-4}
6-MH-AuNPs	367	538	60	1.5×10^{-2}
11-MU-AuNPs	383	502	62	1.2×10^{-2}
11-MUA-AuNPs	375	520	62	3.1×10^{-2}
DT-AuNPs[f]	391	501	60	9.5×10^{-3}

[a] FWHM = full width at half maximum. [b] QYs were determined through comparison with quinine. [c] No absorption band observed. [d] TG = thioglycerol. [e] 4-MB = 4-mercaptobutanol. [f] DT = decanethiol.

AuNPs are 3.1×10^{-2} and 6.2×10^{-5}, respectively. The QY of the 11-MUA-AuNPs is comparable to those of the best currently available water-soluble alkanethiol-protected AuNPs.[4e] Relative to the fluorescence intensity of the as-prepared AuNPs, the fluorescence intensities of the 2-ME-, 6-MH-, and 11-MU-AuNPs are about 100-, 30000-, and 20000-fold higher, respectively. These results suggest that 6-MH and 11-MU are more efficient than 2-ME at minimizing the fluorescence quenching of AuNPs from collisions with quenchers in solution and at minimizing the number of internal nonradiative relaxation pathways. Upon increasing the chain length from six to eleven carbon atoms, we did not observe any increase in fluorescence, which agrees with the previous finding of comparable fluorescence intensities for zeroth-, second-, and fourth-generation PAMAM dendrimer-protected AuNPs.[5a–d]

The fluorescence wavelength underwent a blue shift upon increasing the chain length of the thiol, primarily because of the decreased NP size (Figure 1),[4f,5a] which increased the energy gap between the quantized levels as a result of the smaller core size and the higher coverage of the thiolate.[4f,5a,13] To ensure that these bands were indeed fluorescence signals, we measured the spectra at various concentrations (0.1–200 nM). We observed linear relationships between the signal intensity and the concentration; for example, the

fluorescence intensity of the purified 11-MUA-AuNPs increased linearly over the concentration range from 0.25 to 200 nM, with a limit of detection (LOD) of 0.05 nM (Figure S1 in the Supporting Information). We further studied the behavior of the alkanethiol–AuNPs through measurements of their fluorescence lifetimes. By fitting to a biexponential fluorescence decay (Figure S2 in the Supporting Information), we obtained lifetimes (t_1/t_2) for the 2-ME-, 6-MH-, and 11-MU-AuNPs of 20/158, 27/232, and 45/335 ns, respectively. The monotonical increase in the lifetime upon increasing the length of the thiol chain is consistent with the increasing fluorescence intensities depicted in Figure 2B.

Our synthetic alkanethiol–AuNPs exhibited a number of attractive optical properties. For example, different fluorescence emissions were generated from the various alkanethiol–AuNPs when they were excited simultaneously at a single wavelength ($\lambda_{ex} = 365$ nm). Because the fluorescent AuNPs possess long fluorescence lifetimes (greater than 20 ns), they have great potential for use in sensing molecules of interest through monitoring of their time-resolved fluorescence.[14] The fluorescent AuNPs have large Stokes shifts (greater than 130 nm), which can prevent spectral cross-talk and, thus, enhance the detection signal. The inherent brightness (the bright colors detected under UV-lamp illumination; Figure 2B) allows imaging of a single AuNP, suggesting that they may be applicable to cell imaging.[15] Much like semiconductor quantum dots (QDs), the highly size-dependent fluorescence properties of the AuNPs are very sensitive to the environment.[15,16] Unlike semiconductor QDs, however, the QYs of the fluorescent AuNPs are lower. Nevertheless, the fluorescent AuNPs are easily prepared, with good batch-to-batch reproducibility (relative standard deviation less than 5% from 10 batches) in terms of their fluorescence intensity, and have low toxicity.[17] Although the QYs of the thus-prepared fluorescent AuNPs are lower than those of PAMAM dendrimer-protected Au clusters (smaller than Au_{40}), the thiol–AuNPs (of approximate size Au_{250} for 11-MUA-AuNPs) are readily purified or separated from other matrix components through simple centrifugal filtration (membrane cut-off: 10 kDa).

Next, we tested the practicality of using 11-MUA-AuNPs for sensing Hg^{II}. Mercury pollutants exert adverse effects on the environment and on human health, and thus many methods have been developed for sensing Hg^{II}.[18–22] Based on our experience,[23] lower concentrations of AuNPs often provide better sensitivity for the detection of metal ions. We first investigated the 11-MUA-AuNPs at a concentration 1.0 μM for sensing Hg^{II}. Figure 3 presents the absorption spectra, TEM images, and fluorescence spectra of the 1.0 μM 11-MUA-AuNPs in the absence and presence of 10 μM Hg^{II}. For the first time, we observed aggregation-induced fluorescence quenching of 11-MUA-AuNPs by Hg^{II} in aqueous solution (Figure 3B). The TEM image of aggregated 11-MUA-AuNPs (inset, Figure 3A) supports the notion that the fluorescence quenching phenomenon occurred through Hg^{II}-induced aggregation. The aggregation was due mainly to the interaction of Hg^{II} ions with the carboxylate groups present on the surfaces of the 11-MUA-AuNPs. The 11-MUA-AuNPs are aggregated in solution in the presence of divalent metal

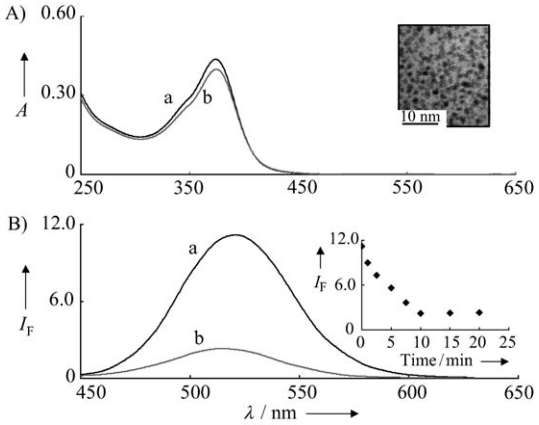

Figure 3. A) UV/Vis absorption and B) fluorescence spectra of solutions containing 11-MUA-AuNPs in the a) absence and b) presence of Hg^{II}. Inset to (A): HRTEM image of 11-MUA-AuNPs in the presence of Hg^{II}. Inset to (B): Time-course measurement of the fluorescence intensity at 520 nm for 11-MUA-AuNPs after the addition of Hg^{II}. Buffer: 5 mM sodium tetraborate solution (pH 9.2); excitation wavelength: 375 nm.

ions through an ion-templated chelation process.[22,23b] By monitoring the decrease in fluorescence, we found that the Hg^{II}-induced aggregation of the 11-MUA-AuNPs reached completion within 10 min (inset, Figure 3B). Although the Hg^{II}-induced fluorescence quenching was quite significant, the effect on the wavelength of absorption was small (Figure 3A); namely, the fluorescence was more sensitive to changes in the AuNP size than the absorption wavelength was. Unlike the absorption of large AuNPs, which is due to SPR, the absorption of small AuNPs is due to metal-centered (Au $5d^{10}$ to 6sp interband transitions) and/or ligand–metal charge-transfer transitions.

We further investigated the changes in fluorescence of the 11-MUA-AuNPs (10 nM) that occurred within 10 min of adding the following metal ions (500 nM): Li^+, Na^+, K^+, Mg^{II}, Ca^{II}, Sr^{II}, Ba^{II}, Cu^{II}, Co^{II}, Ni^{II}, Zn^{II}, Pb^{II}, Hg^{II}, Cd^{II}, Fe^{II}, Al^{III}, Cr^{III}, and Au^{III}. As exhibited in Figure 4, other than Hg^{II},

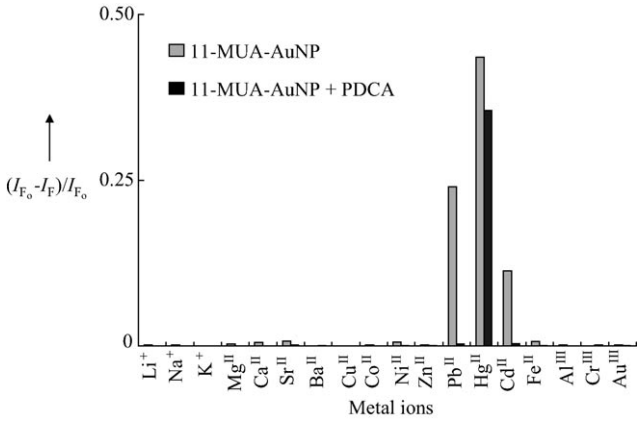

Figure 4. Fluorescence ratios $[(I_{F_0}-I_F)/I_{F_0}]$ at 520 nm for the 11-MUA-AuNPs (10 nM) measured in the absence and presence of PDCA (1.0 mM) after the addition of 500 nM metal ions in 5 mM sodium tetraborate solutions at pH 9.2. Other conditions were the same as those described in Figure 3.

only Pb^{II} and Cd^{II} ions led to great decreases in the fluorescence intensity. The highest fluorescence-decreased response of the probe for Hg^{II} among the metal ions is consistent with the much higher affinity of simple carboxylic acids towards aqueous Hg^{II} ($\log\beta_4 = 17.6$).[24] To further improve the selectivity of the 11-MUA-AuNP probe toward Hg^{II}, we added a chelating ligand, PDCA (1.0 mM), to the solutions, which showed its effective masking ability for Pb^{II} and Cd^{II}.[23] PDCA forms much more stable complexes with heavy metal ions, such as Hg^{II} ($\log\beta_2 = 20.28$), than with other metal ions.[25] The fluorescence intensity of the 11-MUA-AuNPs increased by about 5% (data not shown) in the presence of 1.0 mM PDCA, indicating that some of the PDCA ligands had adsorbed onto the 11-MUA-AuNP surfaces. Thus, we suggest that PDCA improves the probes' selectivity toward Hg^{II} ions through a cooperative effect.[23,26] Furthermore, the PDCA ligands in the bulk solution may form complexes with the other metal ions, suppressing their interference with the probe.[23] As a result, even in the presence of metal ions (other than Pb^{II} and Cd^{II}) at concentrations 400 times greater than that of Hg^{II}, the selectivity of the 11-MUA-AuNPs toward Hg^{II} was maintained. We performed a series of competitive experiments to test the practicality of our 11-MUA-AuNP nanosensor for the selective detection of Hg^{II}. The tolerance concentrations of Pb^{II} and Cd^{II} when sensing Hg^{II} using this 11-MUA-AuNP nanosensor were at least 10 times the Hg^{II} concentrations (Figure S3 in the Supporting Information).

As indicated in Figure 5, the fluorescence of the 11-MUA-AuNPs (10 nM) decreased upon increasing the concentration of Hg^{II} ions. A linear relationship ($R^2 = 0.96$) exists between the value of the fluorescence decrease of the 11-MUA-AuNPs with the logarithm of the concentration of Hg^{II} ions over the range from 10 nM to 10 μM. The LOD for Hg^{II}, at a signal-to-noise ratio of 3, was 5.0 nM (1.0 ppb), which is lower than the maximum level (2.0 ppb) of mercury in drinking water permitted by the United States Environmental Protection Agency (EPA). This approach provides a sensitivity that is two orders of magnitude lower than those reported for heavy metal ion sensors based on chelation/aggregation-mediated colorimetry and AuNP systems based on modulation of fluorescence quenching.[22,27]

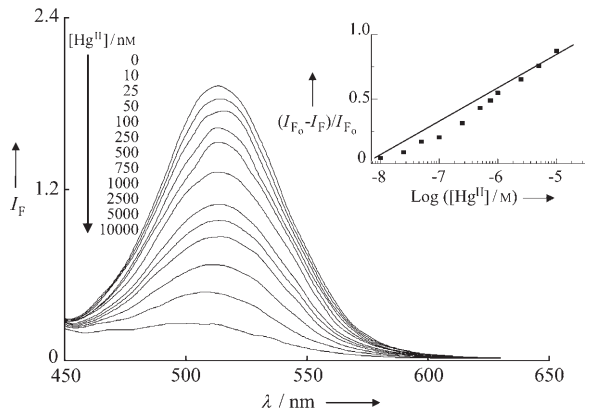

Figure 5. Fluorescence response of 11-MUA-AuNPs upon the addition of Hg^{II} ions (0, 10, 25, 50, 100, 250, 500, 750, 1000, 2500, 5000, and 10000 nM). Inset: Plot of fluorescence ratios $[(I_{F_0}-I_F)/I_{F_0}]$ of 11-MUA-AuNPs at 520 nm versus $\log[Hg^{II}]$. Buffer: 5 mM sodium tetraborate solution (pH 9.2) containing PDCA (1.0 mM).

To test the potential of our Hg^{II}-based nanosensor for the analysis of Hg^{II} in environmental samples, we tested a water sample obtained from a pond on our campus. By applying a standard addition method over a concentration range of 5–100 nM Hg^{II} ($y = 0.29x + 2.25$; $R^2 = 0.98$), we determined the concentration of Hg^{II} in the pond sample to be 3.49 ppb, which is in good agreement with that (3.20 ppb) determined using inductively coupled plasma mass spectrometry (ICP-MS) analysis. The recoveries of these measurements were 95–98%. Our results suggest that this probe has great potential for determining environmentally relevant concentrations of Hg^{II}.

In conclusion, we have created a series of novel, water-soluble, alkanethiol–AuNPs whose fluorescence wavelength is tunable through modification of the chain length of the alkanethiols. The highly fluorescent alkanethiol–AuNPs, such as the 11-MUA-AuNPs (approximate size Au_{250}), are easily purified and are capable of sensing Hg^{II} ions. To the best of our knowledge, this work provides the first example of a system for sensing Hg^{II} ions based on fluorescence quenching through Hg^{II}-induced aggregation of AuNPs. Under the optimum conditions, the sensitivity of the 11-MUA-AuNPs toward Hg^{II} is high (LOD = 5.0 nM), with remarkable selectivity over other metal ions in aqueous solution.

Received: February 22, 2007
Published online: August 2, 2007

Keywords: fluorescence · gold · mercury · nanostructures · sensors

[1] a) M. Brust, M. Walker, D. Bethell, D. J. Schiffrin, R. Whyman, *J. Chem. Soc. Chem. Commun.* **1994**, 801–802; b) A. C. Templeton, W. P. Wuelfing, R. W. Murray, *Acc. Chem. Res.* **2000**, *33*, 27–36; c) U. Drechsler, B. Erdogan, V. M. Rotello, *Chem. Eur. J.* **2004**, *10*, 5570–5579.

[2] S. Link, M. A. El-Sayed, *Annu. Rev. Phys. Chem.* **2003**, *54*, 331–366.

[3] a) S. Chen, R. S. Ingram, M. J. Hostetler, J. J. Pietron, R. W. Murray, T. G. Schaaff, J. T. Khoury, M. M. Alvarez, R. L. Whetten, *Science* **1998**, *280*, 2098–2101; b) J. Zheng, R. M. Dickson, *J. Am. Chem. Soc.* **2002**, *124*, 13982–13983; c) H.-G. Boyen, G. Kästle, F. Weigl, P. Ziemann, *Phys. Rev. Lett.* **2001**, *87*, 276401.

[4] a) S. Link, M. A. El-Sayed, T. G. Schaaff, R. L. Whetten, *Chem. Phys. Lett.* **2002**, *356*, 240–246; b) T. Huang, R. W. Murray, *J. Phys. Chem. B* **2001**, *105*, 12498–12502; c) Y. Yang, S. Chen, *Nano Lett.* **2003**, *3*, 75–79; d) Y. Negishi, T. Tsukuda, *Chem. Phys. Lett.* **2004**, *383*, 161–165; e) G. Wang, T. Huang, R. W. Murray, L. Menard, R. G. Nuzzo, *J. Am. Chem. Soc.* **2005**, *127*, 812–813; f) Y. Negishi, K. Nobusada, T. Tsukuda, *J. Am. Chem. Soc.* **2005**, *127*, 5261–5270; g) G. Wang, R. Guo, G. Kalyuzhny, J.-P. Choi, R. W. Murray, *J. Phys. Chem. B* **2006**, *110*, 20282–20289.

[5] a) J. Zheng, C. Zhang, R. M. Dickson, *Phys. Rev. Lett.* **2004**, *93*, 077402; b) J. Zheng, J. T. Petty, R. M. Dickson, *J. Am. Chem.*

Soc. **2003**, *125*, 7780 – 7781; c) M. L. Tran, A. V. Zvyagin, T. Plakhotnik, *Chem. Commun.* **2006**, 2400 – 2401; d) X. Shi, T. R. Ganser, K. Sun, L. P. Balogh, J. R. Baker, Jr., *Nanotechnology* **2006**, *17*, 1072 – 1078; e) H. Duan, S. Nie, *J. Am. Chem. Soc.* **2007**, *129*, 2412 – 2413.
[6] T. G. Schaaff, R. L. Whetten, *J. Phys. Chem. B* **2000**, *104*, 2630 – 2641.
[7] J. Zhang, S. Xu, E. Kumacheva, *Adv. Mater.* **2005**, *17*, 2336 – 2340.
[8] T. G. Schaaff, G. Knight, M. N. Shafigullin, R. F. Borkman, R. L. Whetten, *J. Phys. Chem. B* **1998**, *102*, 10643 – 10646.
[9] Y. Shichibu, Y. Negishi, T. Tsukuda, T. Teranishi, *J. Am. Chem. Soc.* **2005**, *127*, 13464 – 13465.
[10] P.-A. Buffat, M. Flüeli, R. Spycher, P. Stadelmann, J.-P. Borel, *Faraday Discuss.* **1991**, *92*, 173 – 187.
[11] a) D. Krüger, H. Fuchs, R. Rousseau, D. Marx, M. Parrinello, *J. Chem. Phys.* **2001**, *115*, 4776 – 4786; b) M. Konôpka, R. Rousseau, I. Štich, D. Marx, *J. Am. Chem. Soc.* **2004**, *126*, 12103 – 12111.
[12] a) J. M. Forward, D. Bohmann, J. P. Fackler, Jr., R. J. Staples, *Inorg. Chem.* **1995**, *34*, 6330 – 6336; b) A. Vogler, H. Kunkely, *Coord. Chem. Rev.* **2001**, *219–221*, 489 – 507.
[13] W. A. de Heer, *Rev. Mod. Phys.* **1993**, *65*, 611 – 676.
[14] M. Dahan, T. Laurence, F. Pinaud, D. S. Chemla, A. P. Alivisatos, M. Sauer, S. Weiss, *Opt. Lett.* **2001**, *26*, 825 – 827.
[15] A. P. Alivisatos, W. Gu, C. Larabell, *Annu. Rev. Biomed. Eng.* **2005**, *7*, 55 – 76.
[16] R. E. Bailey, A. M. Smith, S. Nie, *Phys. E* **2004**, *25*, 1 – 12.
[17] R. Hardman, *Environ. Health Perspect.* **2006**, *114*, 165 – 172.
[18] T. Morris, G. Szulczewski, *Langmuir* **2002**, *18*, 5823 – 5829.
[19] E. M. Nolan, M. E. Racine, S. J. Lippard, *Inorg. Chem.* **2006**, *45*, 2742 – 2749.
[20] Y. Tang, F. He, M. Yu, F. Feng, L. An, H. Sun, S. Wang, Y. Li, D. Zhu, *Macromol. Rapid Commun.* **2006**, *27*, 389 – 392.
[21] A. Ono, H. Togashi, *Angew. Chem.* **2004**, *116*, 4400 – 4402; *Angew. Chem. Int. Ed.* **2004**, *43*, 4300 – 4302.
[22] Y. Kim, R. C. Johnson, J. T. Hupp, *Nano Lett.* **2001**, *1*, 165 – 167.
[23] a) C.-C. Huang, H.-T. Chang, *Anal. Chem.* **2006**, *78*, 8332 – 8338; b) C.-C. Huang, H.-T. Chang, *Chem. Commun.* **2007**, 1215 – 1217.
[24] F. M. M. Morel in *Principles of Aquatic Chemistry*, Wiley-Interscience, New York, **1983**, p. 248 – 249.
[25] E. Norkus, I. Stalnionienė, D. C. Crans, *Heteroat. Chem.* **2003**, *14*, 625 – 632.
[26] S.-Y. Lin, C.-H. Chen, M.-C. Lin, H.-F. Hsu, *Anal. Chem.* **2005**, *77*, 4821 – 4828.
[27] a) X. He, H. Liu, Y. Li, S. Wang, Y. Li, N. Wang, J. Xiao, X. Xu, D. Zhu, *Adv. Mater.* **2005**, *17*, 2811 – 2815; b) A. Sugunan, C. Thanachayanont, J. Dutta, J. G. Hilborn, *Sci. Technol. Adv. Mater.* **2005**, *6*, 335 – 340.

